Chinese Chemical Letters 31 (2020) 1616–1619

Contents lists available at ScienceDirect

Chinese Chemical Letters

journal homepage: www.elsevier.com/locate/cclet

Communication

Near infrared molybdenum oxide quantum dots with high photoluminescence and photothermal performance

Xiaoxiao Dong[a], Hong Zhao[a,*], Yuanyuan Mi[a], Yao Liu[b], Yida Zhang[a], Ya Liu[a], Yusheng Chen[c], Quan Xu[a,*]

[a] State Key Laboratory of Heavy Oil Processing, College of Mechanical and Transportation Engineering, China University of Petroleum-Beijing, Beijing 102249, China
[b] Research Institute for New Materials Technology, Chongqing University of Arts and Science, Chongqing 402160, China
[c] Department of Chemical Science, University of Akron, Akron, OH 44325, United States

ARTICLE INFO

Article history:
Received 30 October 2019
Received in revised form 5 November 2019
Accepted 7 November 2019
Available online 9 November 2019

Keywords:
Molybdenum oxide quantum dots
Fluorescence imaging performance
Photothermal performance
Carbon dots
Near infrared

ABSTRACT

The synthesized near infrared molybdenum oxide quantum dots perform excellent red fluorescence imaging performance and photothermal performance, which have 600, 650 and 700 nm three unique peaks excited at 540 nm, with a high quantum yield around 20%. Meanwhile, with 808 nm NIR laser excitation, 10 mg/mL modified Molybdenum oxide quantum dots can increase temperature up to 72.2 °C within 150 s and 77.7 °C within 270 s, respectively.

Two dimensions materials beyond graphene have gain great interest in recent years for their unique mechanical, electrical and chemical properties and have shown great potential in catalysis, phototherapy, bioimaging and sensors applications, *etc.* [1–8]. Two dimension quantum dots (2D-QDs), an emerging and exciting confined 2D nanosheet materials with outstanding photoluminescent and photothermal properties, are one of the rising stars in 2D materials family and have triggered widespread applications in energy, nanomedicine and physical fields [9–17].

Molybdenum oxide quantum dots (MoO_3 QDs) is one of the 2D-QDs reported in recent years and attract scientists for their excellent localized surface plasmon resonance (LSPR) properties with promising application in surface-enhanced Raman spectroscopy (SERS) field [18]. Besides, their widespread absorption wavelength could open their new era in photothermal and phototherapy fields. Although great progress has been made, there is no reported MoO_3 QDs with both effective photothermal and highly photoluminescent properties and thus impede their application in nanomedicine and bioimaging fields.

Here, for the first time, we reported a novel and straightforward strategy of preparing the modified MoO_3 QDs with both high photothermal and photoluminescent properties. The modified MoO_3 QDs shows excitation wavelength from 430−610 nm and emission wavelength at 550−750 nm with quantum yield (QY) up to 20%. To our knowledge, this is the first reported modified MoO_3 QDs with both fluorescence and photothermal properties. The structure of the modified MoO_3 QDs was further explored with X-ray photoelectron spectroscopy (XPS), Fourier Transform infrared spectroscopy (FTIR) and extended X-ray absorption fine structure (EXAFS) and it was founded that local defect and heteroatom doping effect are the major contributors for the outstanding photothermal and photoluminescent properties of modified MoO_3 QDs. This research provided a scope for the commercial application of the modified MoO_3 QDs, especially in nanomedicine and phototherapy field.

The fabrication process is illustrated in Fig. 1. Firstly, MoS_2 powder (50 mg) were sonicated in 30% ethanol solution (10 mL) for 2 h for good dispersion purpose, followed by adding 1.5 mL 30% H_2O_2 to oxidize MoS_2 to MoO_3 (Fig. 1a). With the strong oxidation reactivity of H_2O_2, MoS_2 particle was oxidized to form a loose MoO_3 sheet structure. Heated the autoclave to 40 °C and gradually injected CO_2 into the autoclave until pressure up to 20 MPa, then released CO_2 smoothly at a placid speed after 3 h. With the assistant of CO_2 molecules, proton could further combine with MoO_3 sheet to form $HxMoO_3$ quantum dots. Subsequently, the reacted solution was put into the centrifuge and centrifuged at 6000 rpm for 15 min in order to remove aggregates, and the supernatant was taken as the quantum dots solution prepared.

* Corresponding authors.
E-mail addresses: hzhao_cn@163.com (H. Zhao), xuquan@cup.edu.cn (Q. Xu).

https://doi.org/10.1016/j.cclet.2019.11.010

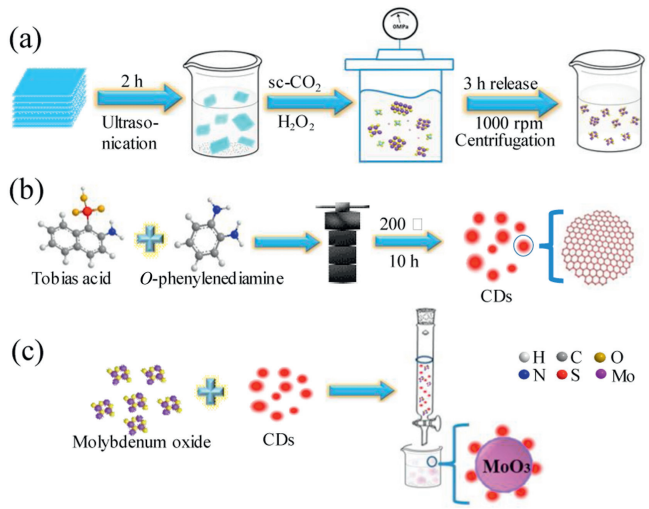

Fig. 1. (a) Schematic illustration of the fabrication process for MoO_3 QDs. (b) Illustration of synthesis process of red carbon dots. (c) Schematic illustration of the preparation process of the MoO_3 QDs grafted red carbon dots.

In the next step, Tobias acid (0.08 g) and *o*-phenylenediamine (0.8 g) were used as precursors, mixed together with ethanol (40 mL) and sealed in a Teflon-lined stainless-steel autoclave to prepare near infrared red CDs (Fig. 1b), which was kept in a furnace at 200 °C for 10 h. Finally, the components of the mixture were further separated by column chromatography. Weighing 22 g silica gel to activate 2 h under 80 °C, dissolved in petroleum ether and packed. Column height is 5 cm. MoO_3 QDs and red CDs were under heat treatment together for 30 min at 60 °C, with the purpose of grafting the MoO_3 QDs edging with red CDs. Then with the roman spectroscopy chromatography purification process, the oversize modified MoO_3 QDs were eliminated and thus the modified MoO_3 QDs with size at 2–10 nm can be obtained. (Fig. 1c).

The morphology of MoO_3 QDs, near infrared red CDs, and modified MoO_3 QDS were characterized by high resolution transmission electron microscopy (HRTEM) images. Fig. 2a reveals the MoO_3 QDs with uniform distribution at size between 2–8 nm. High resolution in Fig. 2b revealed low lattice diffraction fringe, which implied a low degree of the edges of MoO_3 QDs, the fringes with the interplanar spacing of *ca.* 0.35 nm was assigned to the (040) crystal plane of MoO_3 QDs (Fig. 2b) [19]. The HRTEM images of the red CDs were shown in Fig. 2c with uniform distribution sizes with the presence of (100) lattice planes of graphitic carbon with d-spacing ~0.21 nm (Fig. 2d). The modified MoO_3 QDs were shown in Fig. 2e. The sizes of the modified MoO_3 QDs became larger and the fringes lattice were at 0.351 nm (Fig. 2f) which revealed the modified MoO_3 QDs keep the same core of MoO_3 QDs, with enriched oxygen and nitrogen at the edges, which was a critical factor for high photoluminescent function.

To further confirm the MoO_3 core of the modified MoO_3 QDs, we carried out the SEM EDX mapping of the sample and clear Mo, C, O element were observed in Fig. 3a, From Fig. 3a, the chemical elemental distribution was observed *via* SEM-EDX mapping clearly, where the sample of MoO_3 QDs grafted red carbon dots were enrich in Mo, C and O. From the morphology of the modified MoO_3 QDs, carbon and oxygen atom distribution map were well matched with each other, implying the surface of MoO_3 QDs was homogeneously coated with red carbon dots. This was another evidence to prove that red carbon dots were successfully grafted onto MoO_3 QDs. Furthermore, this homogeneously coating was also expected crystallinity with enriched oxygen and hydrogen element at to bring some optical benefit. We further carried out EXAFS spectra in Fig. 3b. The Mo K-edge EXAFS spectra reveal that

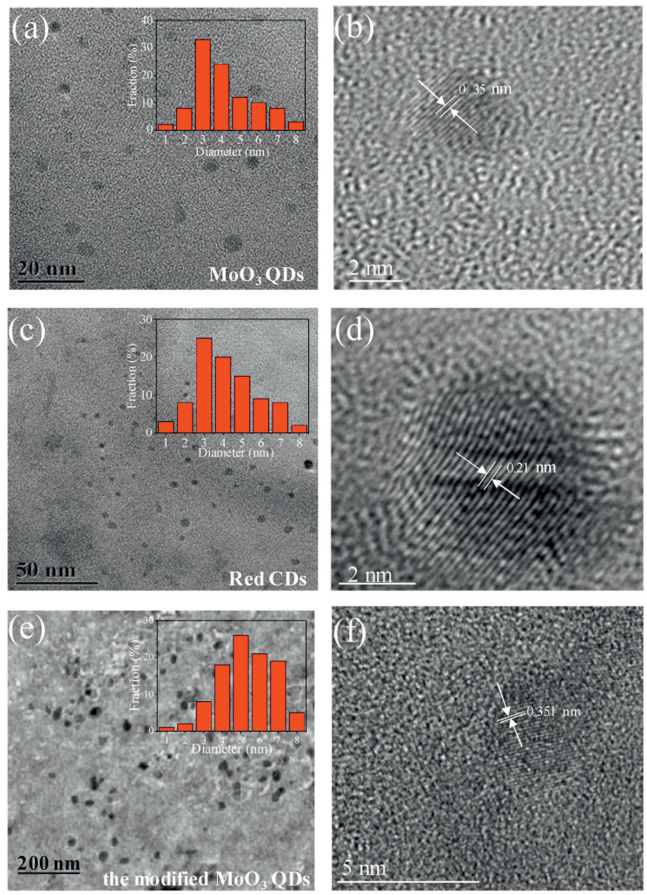

Fig. 2. (a, b) TEM and HRTEM images of MoO_3 QDs. (c, d) TEM and HRTEM images of red CDs. (e, f) TEM and HRTEM images of the modified MoO_3 QDs.

the near-edge absorption energy of Modified MoO_3 dots located between Mo foil and MoO_3, indicated the average electron density around Mo in Modified MoO_3 dots is higher than Mo foil but lower than MoO_3 [20]. It can be further confirmed that the distribution of the modified MoO_3 QDs were uniform and presents lamellar core structure [21]. Several electronic transitions at the absorption edge are strongly dependent on the geometry around the investigated element and can be symmetry forbidden. In Fig. 3b, the pre-edge peak appears as a clear shoulder for Mo oxides, suggesting that Mo atoms are octahedral geometry of MoO_3 in sample modified MoO_3 dots [22].

The photoluminescent of the red CDs and the modified MoO_3 QDs were seen in Figs. 3c and d. In Fig. 3c, it was clearly showed that red carbon dot exhibited three unique photoluminescent peaks at 600, 650 and 720 nm with intensity gradually decreasing. After grafting on MoO_3 QDs, the peak at 720 nm become relatively higher by comparing with peaks at 600 and 650 nm. It is an interesting phenomenon, which indirectly revealed the existence of photoelectron channel and interaction between red carbon dot and MoO_3 QDs. This evidence was consistent with UV absorption results of the MoO_3 QDs were seen in Fig. 3e. After modified with red carbon dots, the absorption peak of the modified MoO_3 QDs was found to be red shifted, which also provided a strong evidence to prove the strong interaction between red carbon dot and MoO_3 QDs. Due to this red shift, it effectively extended the absorption of near infrared range, providing a high photothermal efficiency. The lifetime of MoO_3 QDs and red CDs were shown in Fig. 3f, The lifetime of red carbon dots and the modified MoO_3 QDs diluted 100 times in 99.7% ethanol at room temperature are 15.28 ns, 12.62 ns, respectively. Compared with original MoO_3 QDs, the modified

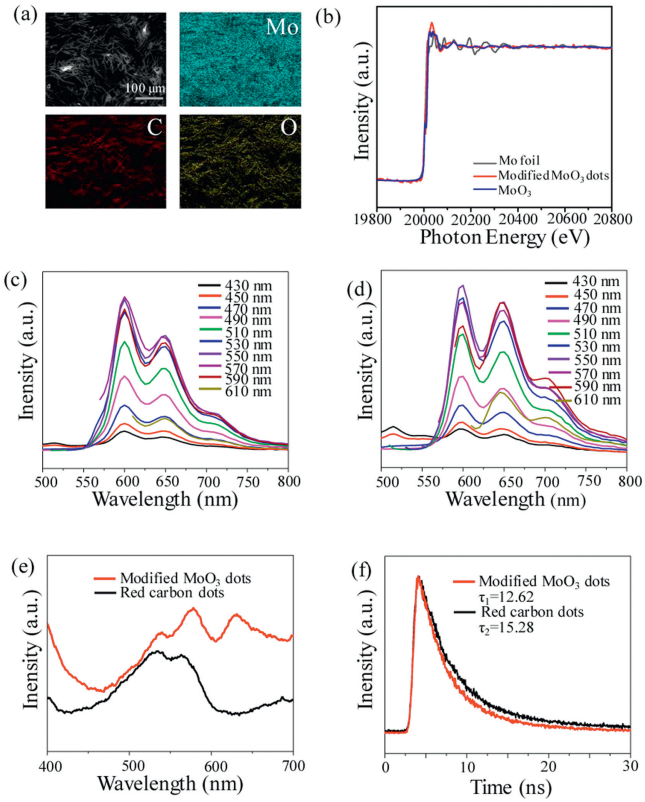

Fig. 3. (a) SEM image of the modified MoO_3 QDs with EDX mapping. (b) The normalized Mo K-edge EXAFS spectra. (c) Photoluminescence spectrum of the red carbon dots. (d) Photoluminescence spectrum of the modified MoO_3 QDs. (e) Absorption spectrum of the red carbon dots and the modified MoO_3 QDs. (f) PL decay spectra of red carbon dots and the modified MoO_3 QDs.

MoO_3 QDs exhibited a shorter lifetime. This can be explained by the existence of photoelectron channel and interaction between red carbon dot and MoO_3 QDs observed in photoluminescent results, which are expected to be benefit for electron-thermal transition for high photothermal efficiency.

When at 540 nm excited, the modified MoO_3 QDs exhibited two peaks at 600 nm and 650 nm respectively, with QY up to 28%. After modification of MoO_3, two peaks were still observed, which indicates that MoO_3 QDs grafted red carbon dots not only preserves the original peaks which means the new material retains the original strong red fluorescence performance, but there also appears a new peak at 700 nm. However, the peak at 700 nm is relatively weak. All of these proved that the modified MoO_3 QDs had excellent fluorescence performance, which broke through the previous lack of fluorescence of MoO_3 QDs.

In order to further prove the strong bonding of chemical elements between the modified MoO_3 QDs after grafting, we conducted XPS test (Figs. 4a and b). At first, from XPS survey spectra of the modified MoO_3 QDs in Fig. S1 (Supporting information) which shows the modified MoO_3 QDs includes mainly chemical elements O, N, C, Mo, S. The element Mo was from 2D material MoO_3 QDs, while the elements N, C, S were from red carbon dots. Fig. 4a is the Mo 3d spectra of the XPS, the peaks at 232.63 and 235.73 eV are ascribed to the $3d_{3/2}$ and the $3d_{5/2}$ orbital electrons of Mo^{6+}, while the peaks at 231.53 and 234.58 eV are attributed to the $3d_{3/2}$ and the $3d_{5/2}$ orbital electrons of Mo^{5+}. According to previous reports, the appearance of Mo^{5+} indicates the interaction between MoO_3 quantum dots and H^+ ions. In our system, the red carbon dots were synthesized in ethanol solvent, when red carbon dots grafted onto the MoO_3 will combination with H^+ in the original system. At the same time, the combination

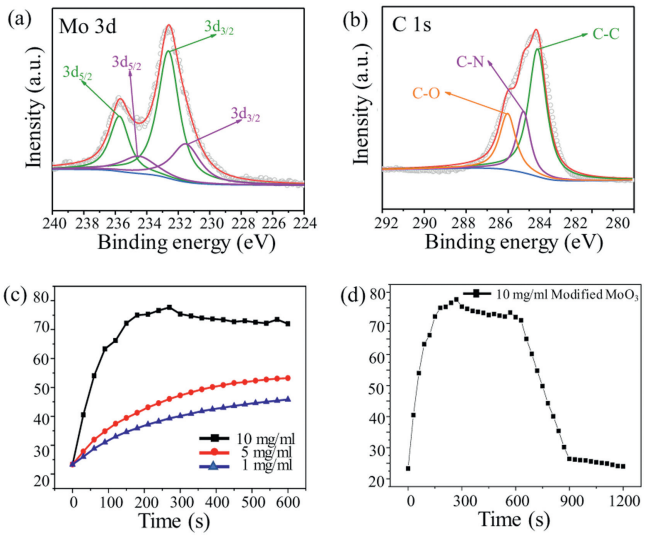

Fig. 4. (a) XPS spectra for Mo 3d in the modified MoO_3 QDs. (b) XPS spectra for C 1s in the modified MoO_3 QDs. (c) Photothermal curves at different concentrations of the modified MoO_3 QDs. (d) Photothermal curve at 10 mg/mL of the modified MoO_3 QDs.

of non-metallic elements in the red carbon dots with molybdenum element will cause the molybdenum ions to lose electrons, so that part of the Mo^{5+} in the system will be converted into Mo^{6+}, which facilitates the formation of lamellar 2D materials [18]. XPS analysis of the C 1s spectra shows the 284.63 eV, 285.28 eV and 286.03 eV binding energy signals referred to C—C, C—N and C—O in Fig. 4b. XPS analysis of the O 1s spectra in Fig. S2a (Supporting information) shows that peaks at 530.78, 531.33, 531.88 and 532.58 eV were attributed to Mo-O, C—O, O—H and C=O, respectively. Fig. S2b (Supporting information) shows that the peak at 399.13 eV was pyridinic N, the peak at 400.53 eV was pyrrolic N, and the peak at 401.38 eV contributed to the graphitic N. We also conducted XRD experiments of MoO_3 and modified MoO_3 to characterize the phase structure in Fig. S3 (Supporting information). From the XRD pattern, we can find the difference between MoO_3 and modified MoO_3 obviously. A clear crystallization formation was found in modified MoO_3, indicating that the modified MoO_3 QDs crystal is more stable [23].

To test the photothermal property of the modified MoO_3 QDs. We conducted photothermal curves of MoO_3 dots at 10 mg/mL, 5 mg/mL and 1 mg/mL respectively (Fig. 4c). The as prepared showed remarkable photothermal property. With an NIR laser at wavelength 808 nm for only 150 s, the 10 mg/mL solution temperature can increase up 72.2 °C. And can further increase to 77.7 °C at 270 s expose time (Fig. 4d). Comparing with previous result, this is the most exciting material both photoluminescent and photothermal properties so far (Table S1 in Supporting information) [24–29]. The electron charge transfer from red CDs to MoO_3 dots was considered as a potential result for this fast speed photothermal property.

To further explain the mechanism, a schematic mechanism was proposed, as shown in Fig. 5. The light with wavelength >430 nm could be converted into photoluminescent with wavelength between 550–750 nm light and emission by red CDs and thus contribute the light property of the modified MoO_3 QDs. And the reset wavelength can be absorbed by red CDs, leading to the charge transfer from red CDs to MoO_3 QDs. And the electron-hole pairs were photogenerated on the surface of MoO_3 QDs [30–32]. In addition, benefited from the heterojunction between MoO_3 QDs and red carbon dots, the modified MoO_3 QDs gained a remarkable photothermal property.

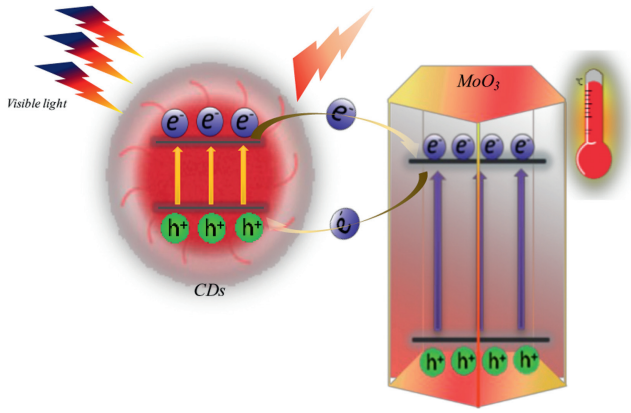

Fig. 5. Proposed photothermal transition mechanism of the modified MoO_3.

Here, for the first time, we fabricated MoO_3 dots with both photothermal and photoluminescent properties. The QY of the modified MoO_3 QDs is nearly 20% with photoluminescent wavelength between 550−750 nm. Significantly, the modified MoO_3 QDs exhibited remarkable photothermal properties in increasing temperature up to 77.7 °C at 270 s with concentration of 10 mg/mL, which made a photothermal record as reported so far. The fast speed electron transfer between red CDs to MoO_3 QDs were considered as one of the main reasons for the photothermal and photoluminescent properties of the modified MoO_3 QDs. With those outstanding properties, the modified MoO_3 QDs are believed to have a great potential in bioimaging and phototherapy field.

Declaration of competing interest

The authors declare that they have no known competing financial interests or personal relationships that could have appeared to influence the work reported in this paper.

Acknowledgements

This work was supported by the National Natural Science Foundation of China (Nos. 51575528, 51875577), Beijing Nova Program Interdisciplinary Studies Cooperative Project (No. Z181100006218138), Science Foundation of China University of Petroleum-Beijing (Nos. 2462019QNXZ02, 2462018BJC004) and the Research Program of Yongchuan Science and Technology Commission (Ycstc, No. 2018nb1402).

Appendix A. Supplementary data

Supplementary material related to this article can be found, in the online version, at doi:https://doi.org/10.1016/j.cclet.2019.11.010.

References

[1] W. Cai, T. Zhang, M. Xu, et al., J. Mater. Chem. C 7 (2019) 2212–2218.
[2] Z.W. Seh, K.D. Fredrickson, B. Anasori, et al., ACS Energy Lett. 1 (2016) 589–594.
[3] Q. Xu, W. Cai, W. Li, et al., Mater. Today Energy 10 (2018) 222–240.
[4] M. Xu, L. Jie, H. Iwai, et al., Sci. Rep. 2 (2012) 406.
[5] H.J. Choi, C.D. Montemagno, Materials 6 (2013) 5821–5856.
[6] Y. Cao, H. Dong, S. Pu, X. Zhang, Nano Res. 11 (2018) 4074–4081.
[7] Y. Chen, Y. Wu, B. Sun, S. Liu, H. Liu, Small 13 (2017) 1603446.
[8] W. Li, Y. Liu, B. Wang, et al., Chin. Chem. Lett. 30 (2019) 2323-2327.
[9] X. Kong, Q. Liu, C. Zhang, et al., Chen, Chem. Soc. Rev. 46 (2017) 2127–2157.
[10] P.V. AshaRani, G.L.K. Mun, M.P. Hande, S. Valiyaveettil, ACS Nano 3 (2009) 279–290.
[11] G. Yang, C. Zhu, D. Du, et al., Nanoscale 7 (2015) 14217–14231.
[12] C. Martin, K. Kostarelos, M. Prato, A. Bianco, Chem. Commun. 55 (2019) 5540–5546.
[13] Y. Feng, B. Gu, Y. Lin, et al., Coord. Chem. Rev. 347 (2017) 77–97.
[14] H. Lin, Y. Chen, J. Shi, Adv. Sci. 5 (2018) 1800518.
[15] S. Lu, B. Yang, Acta Polym. Sin. 7 (2017) 1200–1206.
[16] S. Lu, L. Sui, J. Liu, et al., Adv. Mater. 29 (2017) 1603443.
[17] B. Wang, J. Li, Z. Tang, et al., Sci. Bull. 64 (2019) 1285–1292.
[18] H. Li, Q. Xu, X. Wang, W. Liu, Small 14 (2018) 1801523.
[19] Z. Xie, Y. Feng, F. Wang, et al., Appl. Catal. B: Environ. 229 (2018) 96–104.
[20] W.H. Bing, H. M, et al., Green Chem. 20 (2018) 3071.
[21] T. Ressler, J. Wienold, R.E. Jentoft, et al., Catalysis 210 (2002) 67–83.
[22] G. Poirier, F.C. Cassanjes, Mater. Chem. Phys. 120 (2010) 501–504.
[23] X. Wang, P. Yang, Q. Feng, et al., Polymers 11 (2019) 616.
[24] J. Song, X. Ni, D. Zhang, H. Zheng, Solid State Sci. 8 (2006) 1164–1167.
[25] Q. Xu, M. Xi, C. Liin, et al., Adv. Sci. (2019) 1902043.
[26] S.M. Lam, J.C. Sin, A.Z. Abdullah, A.R. Mohamed, J. Mol. Catal. A: Chem. 370 (2013) 123–131.
[27] D. Ding, W. Guo, C. Guo, et al., Nanoscale 9 (2017) 2020–2029.
[28] W. Liu, X. Li, W. Li, et al., Biomaterials 163 (2018) 43–54.
[29] B. Li, X. Wang, X. Wu, et al., Nanoscale 9 (2017) 11012–11016.
[30] Q. Xu, W. Li, L. Ding, et al., Nanoscale 11 (2019) 1475–1504.
[31] Q. Xu, R. Su, Y. Chen, et al., ACS Appl. Nano Mater. 1 (2018) 1886–1893.
[32] Y. Song, Q. Sun, Briana Aguila, S. Ma, Adv. Sci. 6 (2019) 1801192.